Freezing of gait depends on cortico-subthalamic network recruitment following STN-DBS in PD patients

Gizem Temiz, Marie Des Neiges Santin, Claire Olivier, Antoine Collomb-Clerc, Sara Fernandez-Vidal, Elodie Hainque, Eric Bardinet, Brian Lau, Chantal François, Carine Karachi, et al.

Parkinsonism and Related Disorders xxx (xxxx) 1–9

Contents lists available at ScienceDirect

Parkinsonism and Related Disorders

journal homepage: www.elsevier.com/locate/parkreldis

Freezing of gait depends on cortico-subthalamic network recruitment following STN-DBS in PD patients

Gizem Temiz [a], Marie des Neiges Santin [a], Claire Olivier [a, b], Antoine Collomb-Clerc [a], Sara Fernandez-Vidal [a], Elodie Hainque [a], Eric Bardinet [a], Brian Lau [a], Chantal François [a], Carine Karachi [a, c, 1], Marie-Laure Welter [a, b, d, 1, *]

[a] Inserm 1127, Sorbonne Université, UPMC Univ Paris 06, UMRS 1127, CNRS, UMR 7225, Institut Du Cerveau et de la Moelle Epinière, F-75013, Paris, France
[b] PANAM core Facility, Paris Brain Institute, Paris, France
[c] Neurosurgery Department, AP-HP, Hôpitaux Universitaires Pitié Salpêtrière - Charles Foix, F-75013, Paris, France
[d] Neurophysiology Department, Rouen University Hospital, CHU Rouen, F-76000, Rouen, France

ARTICLE INFO

Keywords:
Parkinson's disease
Deep brain stimulation
Subthalamic nucleus
Freezing of gait
Magnetic resonance imaging
Tractography

ABSTRACT

Introduction: Subthalamic deep-brain-stimulation (STN-DBS) is an effective means to treat Parkinson's disease (PD) symptoms. Its benefit on gait disorders is variable, with freezing of gait (FOG) worsening in about 30% of cases. Here, we investigate the clinical and anatomical features that could explain post-operative FOG.

Methods: Gait and balance disorders were assessed in 19 patients, before and after STN-DBS using clinical scales and gait recordings. The location of active stimulation contacts were evaluated individually and the volumes of activated tissue (VAT) modelled for each hemisphere. We used a whole brain tractography template constructed from another PD cohort to assess the connectivity of each VAT within the 39 Brodmann cortical areas (BA) to search for correlations between postoperative PD disability and cortico-subthalamic connectivity.

Results: STN-DBS induced a 100% improvement to a 166% worsening in gait disorders, with a mean FOG decrease of 36%. We found two large cortical clusters for VAT connectivity: one "prefrontal", mainly connected with BA 8,9,10,11 and 32, and one "sensorimotor", mainly connected with BA 1-2-3,4 and 6. After surgery, FOG severity positively correlated with the right prefrontal VAT connectivity, and negatively with the right sensorimotor VAT connectivity. The right prefrontal VAT connectivity also tended to be positively correlated with the UPDRS-III score, and negatively with step length. The MDRS score positively correlated with the right sensorimotor VAT connectivity.

Conclusion: Recruiting right sensorimotor and avoiding right prefrontal cortico-subthalamic fibres with STN-DBS could explain reduced post-operative FOG, since gait is a complex locomotor program that necessitates accurate cognitive control.

1. Introduction

Deep brain stimulation of the subthalamic nucleus (STN-DBS) has been widely demonstrated to improve Parkinsonian motor disability with dramatic alleviation of rigidity, akinesia and tremor, along with improvement of dopa-related motor complications [1]. A link between dopa-responsiveness and the effects of STN-DBS on akinesia, rigidity and tremor has been well established [2], this feature being the most predictive factor of a good STN-DBS outcome. The effects of STN-DBS on PD gait and balance disorders, and freezing of gait (FOG) are more variable among patients [3–6], and found to be less correlated with their preoperative dopasensitivity. Indeed, FOG improves in about a third of patients, whereas in another third it is rapidly worsened in the year following surgery [4,5]. The factors that contribute to the negative outcome for FOG have not yet been fully identified. Some authors point out the potential role of demographic factors and disease features, in particular old age [2,3], the severity of

* Corresponding author. Neurophysiology Department, CHU Rouen, 1 rue de Germont, 76031, Cedex, Rouen, France.
E-mail address: marielaure.welter@icm-institute.org (M.-L. Welter).
[1] These authors contributed equally.

https://doi.org/10.1016/j.parkreldis.2022.10.002
Received 13 June 2022; Received in revised form 29 September 2022; Accepted 2 October 2022
1353-8020/

gait disorders before surgery [4–6], cognitive deficit [3], and the stimulating contact location or parameter settings [7,8].

More recently, some authors have searched for "sweetspots" for improving the cardinal motor and non-motor signs of PD with STN-DBS, by using MRI approaches and correlation analysis. For the improvement of akinesia and rigidity, a link between the positive effects of STN-DBS was found for a volume of activated tissue (VAT) with a centre of mass (sweetspot) located in the most posterior part of the STN [9,10], and a functional connectivity profile with negative correlations with sensorimotor cortices and positive correlations with specific frontal regions and motor cerebellum [11]. A correlation was also found for non-motor signs, including apathy or depression, and linked to an increase in the left prefrontal connectivity with VAT induced by STN-DBS [12,13]. In a large retrospective cohort study, we found that the sweet spot for improving FOG was located more anteriorly within the STN, roughly corresponding to its centre, just beyond the posterior sensorimotor part of the nucleus [4]. In a recent retrospective study performed on a cohort of 47 PD patients with STN-DBS, a significant correlation between FOG improvement and the recruitment of premotor, motor and prefrontal dorsolateral cortico-subthalamic fibres was also reported [14], suggesting a possible influence of cortico-subthalamic fibres recruitment in post-operative FOG improvement. Taken together, these data suggest that the effects of STN-DBS can be explained by both the modulation of the target site inside the STN and the fibres recruited within the VAT, especially the fibres belonging to the hyperdirect cortico-subthalamic pathway [15]. Nevertheless, the optimal stimulation site for improving gait remains to be prospectively assessed, also using objective assessment, and the potential link between FOG and cortico-subthalamic fibres recruited within the VAT induced by STN-DBS is not fully identified.

Here, we aimed to identify the clinical and diffusion weighted imaging (DWI) factors that could correlate with post-operative FOG severity. For this purpose, we prospectively studied a cohort of 19 PD patients to examine the link between the hyperdirect cortico-subthalamic tracts included in each individual VAT and the effects of STN-DBS on gait and balance disorders including FOG.

2. Patients and methods

This study includes 4 steps:1) we prospectively assessed gait and balance disorders in 19 PD patients before and 6 months after STN-DBS, using validated clinical scales and instrumented gait recordings; 2) we built a PD normative whole brain tractogram using DWI obtained before surgery in another cohort of 33 PD patients not operated but with similar demographic and clinical characteristics; 3) we modelled individual VATs for each hemisphere using the individual DBS parameters for each of the 19 patients; and 4) we normalised all the VATs into a common brain space and searched for potential relationships between the severity of postoperative FOG and the specific cortico-subthalamic streamlines included in each individual VAT.

2.1. Patients

Two separate cohorts of PD patients were included at the Pitié-Salpêtrière Hospital, Paris. A first cohort of 20 PD patients (15 M/5F) candidate for STN-DBS were included for complete pre and post-operative clinical and gait assessments (Table 1). One patient was not operated due to eye infection and therefore excluded. A second cohort of 33 patients with Parkinson's disease (24 M/10F) were included pre-operatively for a 3 T MRI acquisition (Table 1).

Inclusion criteria for both patient groups for STN-DBS in our centre were as follows: (1) age below 70 years; (2) severe form of PD; (3) >50% reduction in motor symptoms On-dopa; and (4) disabling dopa-induced motor complications despite optimal medical treatment. Exclusion criteria were dementia, ongoing psychiatric disturbances, surgical contraindications, and relevant brain lesions detected on MRI [4].

All patients provided their informed written consent in accordance with the declaration of Helsinki, and the local ethics committee approved the study (CPP Ile-de-France Paris VI; INSERM promotion RBM 2012-A00225-38 and 2016-A00231-50; ClinicalTrials.gov: NCT01682668 and NCT02800460).

2.2. Clinical evaluation and gait initiation recordings

In the first cohort of PD patients, clinical assessments and gait recordings were performed: (1) before surgery with no dopaminergic treatment for at least 12 h (Off-dopa) and after a supra-threshold of dopaminergic treatment (On-dopa; usual morning dose + 50 mg), and (2) 6 months after surgery with STN-DBS using chronic individual settings without dopaminergic treatment. We assessed parkinsonian disability with the Unified Parkinson's Disease Rating Scale (UPDRS parts I to IV), gait and balance disabilities with the Gait and Balance Scale (GABS), and FOG severity with the Freezing of Gait Questionnaire (FOG-Q) [16]. Cognitive status was assessed using the Mattis Dementia Rating Scale (MDRS) performed before and after surgery (Table 1).

Table 1
Demographic and clinical characteristics of PD patients with STN-DBS and PD patients with DWI analysis.

	STN-DBS cohort				DWI cohort	
Age (yrs)	58.8 ± 9.9				57.8 ± 10.3	
Disease duration (yrs)	11.7 ± 4.1				11.0 ± 3.1	
	Before surgery		**After surgery with STN-DBS**			
	Off-dopa	**On-dopa**	**Off-dopa**	**On-dopa**	**Off-dopa**	**On-dopa**
Parkinsonian disability						
UPDRS part I		1.1 ± 1.5		0.6 ± 1.3		1.6 ± 1.1
UPDRS part II	20.4 ± 7.2	5.5 ± 4.0	9.2 ± 4.2*	6.6 ± 3.7	20.2 ± 8.8	8.6 ± 6.4
UPDRS part III	37.8 ± 11.7	10.3 ± 7.6	16.8 ± 9.3*	10.6 ± 7.3	38.8 ± 12.0	13.4 ± 8.3
Axial score	6.1 ± 3.5	1.8 ± 1.7	4.6 ± 2.8	2.9 ± 2.4	6.2 ± 3.8	2.8 ± 1.7
UPDRS part IV		8.6 ± 3.9		1.8 ± 1.8*		9.8 ± 4.1
Gait and balance scale	17.3 ± 10.4	4.5 ± 4.4	8.8 ± 6.3*	9.8 ± 4.1		_
FOG-Q		17.5 ± 12.2		10.6 ± 8.3		_
ABC-scale		64.8 ± 21.9		71.0 ± 18.7		_
MDRS		139.6 ± 4.3		137.6 ± 5.0		139.0 ± 3.7
LEDD (mg/d)		1082 ± 351		598 ± 386*		1072 ± 426

*P < 0.05 between before and after surgery with STN-DBS for the same dopa conditions.
ABC: activities balance confidence; FOG-Q: freezing of gait questionnaire; MDRS: Mattis dementia rating scale; LEDD: levodopa equivalent daily dosage; STN-DBS: subthalamic nucleus deep brain stimulation; UPDRS: Unified Parkinson's Disease Rating Scale.

We measured gait initiation parameters using a force platform (0.9 × 1.8 m, AMTI, Advanced Mechanical Technology Inc. Watertown, MA, USA). In order to obtain a better reproducibility of gait recordings, the patient initiated gait barefoot on the platform following an auditory Go signal, walked for 5–6 m, and returned for 15 to 30 trials (Fig. S1) [17]. Gait initiation events for the first two steps were manually identified and the following temporal and spatial parameters calculated: (1) the duration of the anticipatory postural adjustments (APA) and double-stance phases, and (2) the maximum posterior and (3) lateral CoP displacements during the APA, (4) length, (6) width and (7) velocity of the first step [17].

In the second cohort of 33 PD patients, clinical assessment was also performed Off-dopa and On-dopa, and also included the UPDRS parts I to IV, and the MDRS (Table 1).

2.3. Neurosurgical procedure, parameter setting and modelling of the individual volume of activated tissue

The STN was directly targeted using 3D T2 Flair weighted images on the inclusion MRI and indirect targeting using our in-house YeB atlas [4]. The day of the surgery, a pre-operative stereotactic 1.5 T MRI acquisition with T1 weighted images and gadolinium was performed (GE Healthcare, Optima MR 450W, USA) for surgical planning to calculate the target coordinates in the Leksell space and to define trajectories avoiding blood vessels, ventricles and the caudate nucleus. Quadripolar electrodes (Medtronic, 3389-28) were implanted using microelectrode recordings and clinical testing in awake patients, and connected to a pulse generator (Medtronic, Kinetra, Minneapolis). After surgery, the electrode and contact locations were determined using postoperative helical tomography and merged with the preoperative stereotactic MRI. Parameter settings were chosen according to the patient's clinical exam after surgery and adjusted during outpatient visits.

The precise therapeutic contact location was calculated with reference to the posterior commissure [4] and the VATs modelled on the individual MRI using chronic parameter settings for each hemisphere by considering the contact dimensions (1.5 mm height, 1.27 mm diameter) and a homogenous isotropic tissue medium with conductivity of 0.3 S/m, as using PyDBS tool as explained previously [18] by using finite element methods to calculate electrical potentials to determine the neural activation volumes as a function of stimulus parameters and the magnitude of capacitive component of electrode-tissue interface. All the VATs of the 19 patients were then computed and normalised hemisphere by hemisphere within a common space using linear transformation (block-matching algorithm) with 6° of freedom.

2.4. Diffusion weighted imaging data and processing for normative whole brain probabilistic tractography

The 3 T MRI images were acquired using magnetisation-prepared 2 rapid acquisition gradient echo (MP2RAGE) sequences (TR/TE = 5000/3.12, voxel size = 0.9 × 0.9 × 0.9 mm^3) with an acquisition time of 8 min together with a multi shell DWI using a single-shot 2D spin-echo multiband Echo Planar Imaging (EPI) sequence. Each DWI dataset contained 3 shells that were acquired with reverse phase encoding directions (anterior-posterior and posterior-anterior, with b-values of 300, 1000, 2000 s/mm^2 and with respectively 8, 32, and 64 directions per shell with the following parameters: TR/TE = 3500/75, voxel size = 1.76 × 1.76 × 1.76 mm^3). The total acquisition time for the DWI dataset was 12 min. All DWI data were preprocessed in order to remove Rician noise, Gibbs ringing, head motion and susceptibility-based artefacts and eddy current distortion. An additional correction for intensity inhomogeneities was applied (see supplementary methods).

Individual response functions were estimated using multi-shell multi-tissue constrained spherical deconvolution framework and averaged in order to use group-based response functions for different tissues (white matter, grey matter and cerebro-spinal fluid). Fibre orientation distributions (FOD) were calculated for each subject using their individual DWI data and population averaged response functions. Individual FODs were used in order to create PD patient-group specific FOD templates by applying affine and diffeomorphic alignment with MRtrix.

For the segmentation of regions of interest, an anatomical template was also constructed by applying the same transformations to the subjects' T1w images (reconstructed in individual DWI space, and preprocessed with histogram matching). We segmented all 39 cortical Brodmann areas (BA) included in the Brodmann atlas MRIcro (https://www.mccauslandcenter.sc.edu/crnl/mricro) by first linear registration (FLIRT from FSL) followed by a non-linear registration (FNIRT from FSL), and finally adjusting each segmentation to the cortical ribbon computed with Freesurfer. The FOD template was used to reconstruct the whole brain tractography using a probabilistic approach (for details see Ref. [19]). Spherical informed filtering techniques (SIFT2) were applied to the whole brain tractography, in order to compute the weighting factor of each streamline.

2.5. Analysis of cortical connectivity for individual VAT

Each individual VAT of the first cohort was aligned to the normative space and the cortical connectivity of each VAT extracted from the whole brain tractography. Tracks of interest were extracted between each VAT and each cortical region by using whole brain tractography and the corresponding weighting factor. The sum of the weights of each streamline involved in tracks of interest was then calculated. These metrics represent the fibre bundle capacity (FBC) of each tract of interest and provide quantitative information to estimate connectivity.

2.6. Tractography-based STN anatomical-functional subdivisions based on cortical connectivity

The cortico-subthalamic pathway was isolated using normative whole brain tractography, and the cerebellar peduncles, striatum and pallidum were excluded to ensure specificity for the hyperdirect cortico-subthalamic pathway. STN subdivisions were created by measuring similarity between cortical connectivity of STN voxels as previously reported [19]. For this purpose, we first evaluated the optimal number of clusters using the Davies and Bouldin criterion by generating 2 to 6 clusters for the cortical connectivity profile of each voxel located in the STN. Using these criterion, we then determined the number of clusters with the highest similarity score within each cluster and lowest similarity score between clusters (Matlab version 2020b).

2.7. Statistical analysis

For the first cohort of patients, we assessed the changes in parkinsonian disability and gait and balance disorders after STN-DBS relative to baseline (Off-dopa) using Wilcoxon-rank sum tests. We compared the demographic and clinical scores at baseline in patients with a score for FOG-Q greater than or equal to 10 *vs* patients with a score less than 10. Finally, we also compared the demographic and clinical scores between the first and the second cohort of patients using non-parametric Kuskall Wallis tests.

For VAT analysis, we first assessed the correlations between connectivity of each VAT with the 39 BAs using Pearson correlation and clustered the cortical VAT connectivities regarding their intercorrelations (connectivity tendency similarity: co-increase or co-decrease of

connectivity) by Ward's minimum variance method into two clusters. We then summed the connectivity of each VAT within these clusters.

Finally, we examined the correlations between the severity of gait and balance disorders after STN-DBS, and the cortical fibres contained in each VAT using univariate correlations between UPDRS-III, FOG-Q, GABS and MDRS scores. We further examined the correlations using multiple linear regression to include UPDRS-III, FOG-Q, GABS, and MDRS scores as simultaneous explanatory variables. A separate model was fitted for each hemisphere (left and right) and connectivity network (sensorimotor and prefrontal), and we corrected for multiple comparisons to control the false discovery rate. We also assessed the correlation between the clinical scores and the intersected VAT volumes with STN subdivisions in order to analyse spatial information with respect to STN organization. We ran separate multivariate regression models to assess the linear relationship of gait initiation parameters (APA and double-stance durations, step length) after STN-DBS, first with VAT connectivity and then with the intersected VAT volumes with STN subdivisions. A p-value < 0.05 was considered significant.

3. Results

3.1. Effects of levodopa treatment and STN-DBS on parkinsonian disability and gait assessment

Before surgery, 15 out of 19 patients of the first cohort had mild FOG (Fig. 1), and 15/19 recurrent falls (mean [SD] item 13-UPDRS II: 2.3 [1.4]). In these patients, the UPDRS III improved by 75%, the axial score by 71%, and the GABS score by 72% On-versus Off-Dopa (Table 1). Gait kinetics were also significantly improved On-versus Off-dopa, with increases of the step length and velocity, posterior and lateral APA CoP displacements, and decreases of the APAs and double-stance phases (Fig. S2). In the second cohort of 33 PD patients, the UPDRS III improved by 66% and the axial score by 67% On-versus Off-Dopa (Table 1). We found no significant differences in the demographic and clinical features between the first and second cohorts of PD patients (Table 1).

In the first cohort of PD patients, we compared clinical scores with STN-DBS alone to Off-Dopa before surgery, and found that the UPDRS-III score decreased by a mean of 56%, the GABS score by a mean of 49%, and the axial score (including dysarthria) by a mean of 18% (Table 1). Relative to before surgery, the FOG-Q also decreased by a mean of 36% (with usual dopaminergic treatment). Lastly, the LEED decreased by a mean of 43% (Table 1). For gait recordings, we found that the posterior APA CoP displacement, step length and velocity significantly increased (Fig. 1, Fig. S2). The lateral APA CoP displacement, APA and double-stance phase durations were not significantly different (Fig. S2), indicating little or no improvement in postural control.

We observed different effects of STN-DBS on gait and postural control at the individual level, with changes ranging from a 100% improvement to a 166% worsening in the GABS score and a worsening of FOG severity for 5/19 patients (Fig. 1), and, for gait parameters, an absence of increase in the step length in 8/19 patients (Fig. 1). We found no significant differences in the baseline demographic and clinical features between patients with a FOG-Q greater than or equal 10 compared to those with a FOG-Q less than 10 after surgery (Table S1).

3.2. Relationship between therapeutic contact location, VAT cortical connectivity and PD disability

The mean (SD) coordinates of the stimulating contacts were not significantly different between right and left sides (Fig. S3). We found no significant correlation between the therapeutic contact location and the UPDRS-III, FOG-Q, and GABS scores, or gait parameters after surgery (not shown).

The correlation analysis of the connectivity between each VAT showed that the VAT connectivity of the BA 8-11,25,32,35,36 and 45-48 were positively correlated between themselves, and negatively with the BA 1-4,6,7,19-23,34, and 37-41 (Fig. 2A), for both hemispheres. Similarly, the VAT connectivity of the BA 1-4,6,7,19-23,34 and 37-41 were positively correlated between themselves (Fig. 2A). We therefore, separated VAT connectivity into two large clusters: one including predominantly BA 8, 9, 10, 11, 32 named “prefrontal” and one including predominantly BA 1-2-3, 4, 6 named “sensorimotor” (Fig. 2A).

Using univariate correlations between different measures of parkinsonian disability (UPDRS-III, FOG-Q, GABS, MDRS scores), and VAT connectivity profiles, we found significant correlations for prefrontal and sensorimotor VAT connectivity of the right hemisphere ($p = 0.001$, $R^2 = 0.62$; and $p = 0.046$, $R^2 = 0.33$; for right prefrontal and right sensorimotor connectivity, respectively, Fig. 2B). Multiple linear regression analysis confirmed the univariate correlation with a significant positive association between FOG severity and right prefrontal VAT connectivity (FOG-Q; semi-partial correlation = 0.58, adjusted $p = 0.0027$), and a significant negative corre-

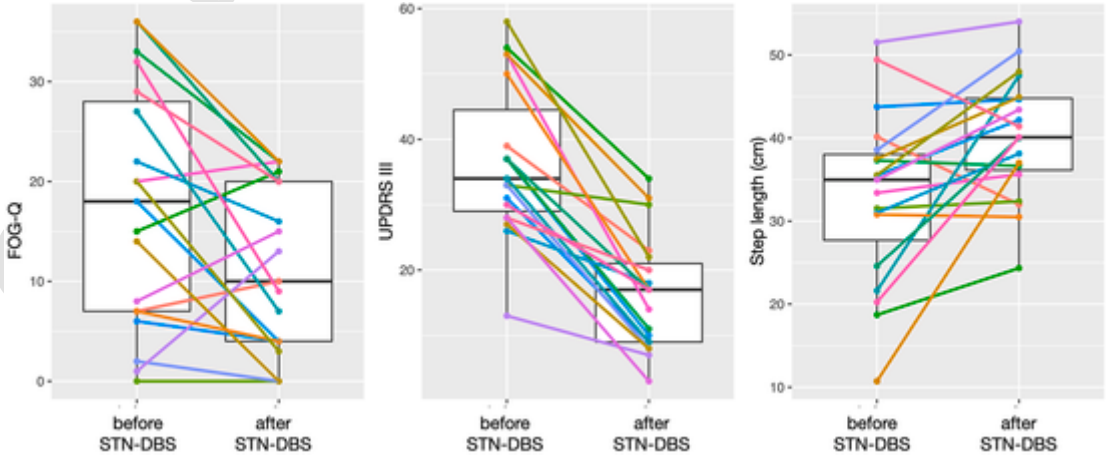

Fig. 1. Effects of STN-DBS on freezing of gait, parkinsonian disability, and step length
The graphs show the changes in the freezing of gait questionnaire (FOG-Q, On-dopa, left panel), UPDRS-III score (Off-dopa, middle panel) and step length (Off-dopa, right panel) before and after subthalamic deep brain stimulation (STN-DBS). The box plots show upper and lower quartiles and median of these observations. Each colour point represents an individual patient. .(For interpretation of the references to colour in this figure legend, the reader is referred to the Web version of this article.)

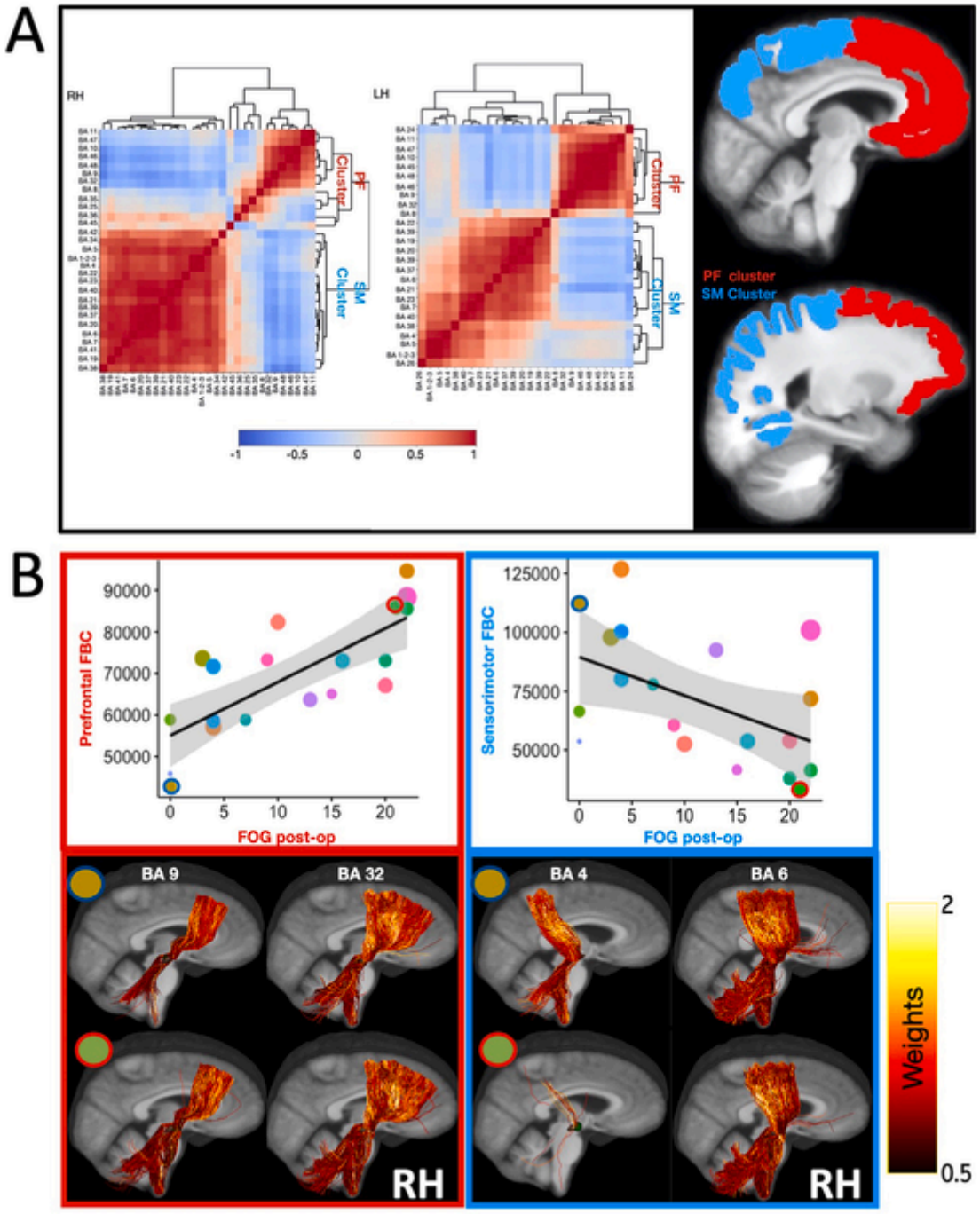

Fig. 2. Inter-correlations between cortical connectivity of VATs and relationship with FOG severity after surgery
A. Left: Inter-correlations between the cortical connectivity for volume of activated tissues (VATs) for the right and left hemispheres (RH and LH, left and right panels, respectively). Right: visualisation on the template space of the VAT prefrontal (PF, red) and sensorimotor (SM, blue) clusters of the right hemisphere on sagittal (top) and lateral (bottom) views.B. The graphs show the bivariate relationship between the postoperative FOG-Q score and the VAT connectivity of the prefrontal cortex represented as fibre bundle capacity (upper left panel) and those of the sensorimotor cortex (upper right panel) in the right hemisphere (RH). The regression line is in black and the 95% confidence interval in grey, and each coloured dot represents individual VATs of each patient, and the dot size is proportional to its volume. The blue framed dot shows the VAT connectivity of one patient without FOG after surgery and the red framed dot represents the VAT connectivity of one patient with severe postoperative FOG. Heat colour map of the streamlines represents weight of the streamlines. (For interpretation of the references to colour in this figure legend, the reader is referred to the Web version of this article.)

lation between FOG severity and right sensorimotor VAT connectivity (semi-partial correlation = −0.55, adjusted p = 0.023).

3.3. Relationship between intersected VAT and STN subdivision in relation to PD disability

Based on cortico-subthalamic connectivity, we found that the STN could be divided into two subdivisions: one posterior that mainly connected the sensorimotor areas (BA 4, 6), and one anterior that mainly connected the prefrontal areas (BA 8, 9, 10 and 32) for both hemispheres with a smooth gradient of change of connectivity between them (Fig. 3A). However, we found size differences for the sensorimotor and the prefrontal subdivisions occupying respectively 55% and 45% for the right STN, and 77% and 23% for left STN (Fig. S5).

We found that the overlap between the VAT and the right sensorimotor STN subdivision was significantly correlated (p = 0.009; R^2 = 0.47), and negatively with post-operative FOG severity (FOG-Q score, ß = −1.69, p = 0.0017, Fig. 3B).

For gait parameters, we found a significant negative correlation between the overlap between the VAT and the left sensorimotor STN subdivision (p = 0.02, R^2 = 0.35) and the post-operative double stance duration (ß = −230.8, p = 0.037), and a significant positive correlation with the post-operative APA duration (β = 151.8, p = 0.018) (Fig. S6).

4. Discussion

In this study, we found a significant link between cortico-subthalamic fibres recruitment and post-operative FOG severity in PD patients with STN-DBS. Using PD DWI data, we found that lower post-operative FOG severity correlated with a higher connectivity of the individual VAT induced by STN DBS with the right sensorimotor cortical areas and with a VAT located more posterior within the right STN. Conversely, more severe post-operative FOG correlated with a higher VAT connectivity with the right prefrontal cortical areas. We also found that better post-operative executive functions correlated with a higher VAT connectivity with the right sensorimotor cortical areas.

In these PD patients that have mild axial motor symptoms that respond to dopaminergic treatment before surgery, we observed differential effects of STN-DBS on gait and balance at the individual level, with, for some patients a dramatic alleviation of gait after STN-DBS whereas an aggravation was observed in about 1/3 of patients [4–6], with no difference at baseline between “freezers” and “non-freezers” patients. This confirms that a good response to dopaminergic treatment before surgery does not guarantee a good outcome of axial motor symptoms after STN-DBS [3,20]. Interestingly, gait recordings showed that STN-DBS improved forward gait parameters (such as walking velocity) but not the postural and preparatory phases of gait (such as double stance and APA durations). This result suggests that STN-DBS has a positive impact on the akinetic gait components but may modify the functional network involved in more complex motor programs, including gait initiation and postural control [21]. Such differential effects of STN-DBS on gait and posture have been previously reported in PD patients, with an alteration of dual-task walking with STN-DBS [8], also identified as a driver for the occurrence or FOG aggravation [22–24]. This suggests that STN-DBS, especially when recruiting prefrontal-subthalamic fibres, could negatively influence executive functions [25], and, in consequence, FOG. In line with this hypothesis, we found that the severity of FOG after surgery was linked to a higher VAT connectivity with the prefrontal cortico-subthalamic pathway. However, this relationship was observed independently of cognitive status (quantified by MDRS score) suggesting that the modulation of these cortico-subthalamic tracts participate in post-operative FOG. This prefrontal network includes the frontal eye field (area 8), the dorsolateral prefrontal (area 9), anterior prefrontal (area 10), the dorsal anterior cingulum (area 32), and weakly the frontal orbital (area 47) cortices. These brain areas are involved in cognitive information processing, such as complex movement planning, action control and working memory [26,27]. Recent imaging studies performed in PD patients with FOG showed a decrease of cortical thickness in the orbital, prefrontal dorsolateral and anterior cingulum cortices [28]. These data suggest that STN-DBS modifies the functioning of non-motor cortico-STN pathways which could result in an impairment of some complex aspects of gait control.

Conversely, lower FOG severity was related to a higher connectivity of the VAT with sensorimotor cortices (mainly BA 1, 2, 3, 4, 6 and 8), which have been widely demonstrated to be activated in the preparation and execution phases of movement, including gait [29]. This result is in accordance with the recent report of a significant link between FOG improvement after STN-DBS and a higher connectivity with motor and premotor cortico-subthalamic fibres [14], as also reported for other parkinsonian motor signs, such as rigidity or akinesia [10]. In PD patients with STN-DBS, PET imaging also suggested that FOG severity improvement was associated with metabolic activity changes in sensory associative cortices [30]. Interestingly in our patients, the intersected VAT connectivity within the STN for lower FOG severity was not only located in the dorsolateral part of the nucleus, as reported by others for akinesia [9,10], but towards its centre which roughly corresponds to the sweet spot for FOG that we previously obtained in our large retrospective cohort [4]. This spot is located within the STN at the junction between the motor and associative subparts of the GPe-STN projections (defined previously in monkeys) and also at the junction between the sensorimotor and prefrontal cortico-subthalamic tracts in the right hemisphere, suggesting that FOG improvement may be linked to the combined modulation of mainly sensorimotor cortico-STN tracts and associative GPe-STN connections. However, our DWI technique does not allow to study the influence of other basal ganglia-mesencephalic locomotor networks with high reliability mainly because of the large number of fibres crossing towards the STN and the GPe, pedunculopontine (PPN) and cuneiform nuclei. It is also possible that STN-DBS altered or alleviated the functioning of other pathways involved in gait control such as PPN-STN fibres, known to be altered in PD with dopa-resistant FOG [31], or lenticular fasciculus fibres as recently suggested in a retrospective study [14]. Lastly, the effects of STN-DBS could also be related to the abnormal STN neuronal activity patterns observed in PD patients with increased beta band activity previously found in freezers PD patients at rest or during arrests of stepping movements [32].

We observed differences for correlation for the right and left VAT connectivity, with significant results only for the right hemisphere. This could be explained by the different volumes of the sensorimotor and the prefrontal subdivisions of the right and left STN, with a larger left sensorimotor STN subdivision and therefore a smaller intersected VAT with the small left prefrontal STN subdivision. Another possibility would be that right and left STN have distinct influences on locomotion, as reflected by their distinct cortico-subthalamic connectivity, with a pre-eminence of the right STN for gait control as observed using functional MRI in healthy controls [33], and the observation of asymmetric PPN connectivity in PD patients with FOG [34]. Some recent studies have examined the impact of asymmetric STN-DBS for improving FOG in PD patients [35]. The published data are however contradictory up to now. In a recent randomized cross-over study, reducing left STN-DBS amplitude by 50% was found to decrease axial motor signs and FOG-Q, but no significant change was found when reducing the right STN-DBS amplitude [36]. In another randomized study, reducing stimulation amplitude by 30% contralateral to the least affected side had no positive effect with conversely an aggravation of symptoms, leading to a premature drop-out for 8/12 patients [37]. Lastly, comparing unilateral right and left side STN-DBS effects

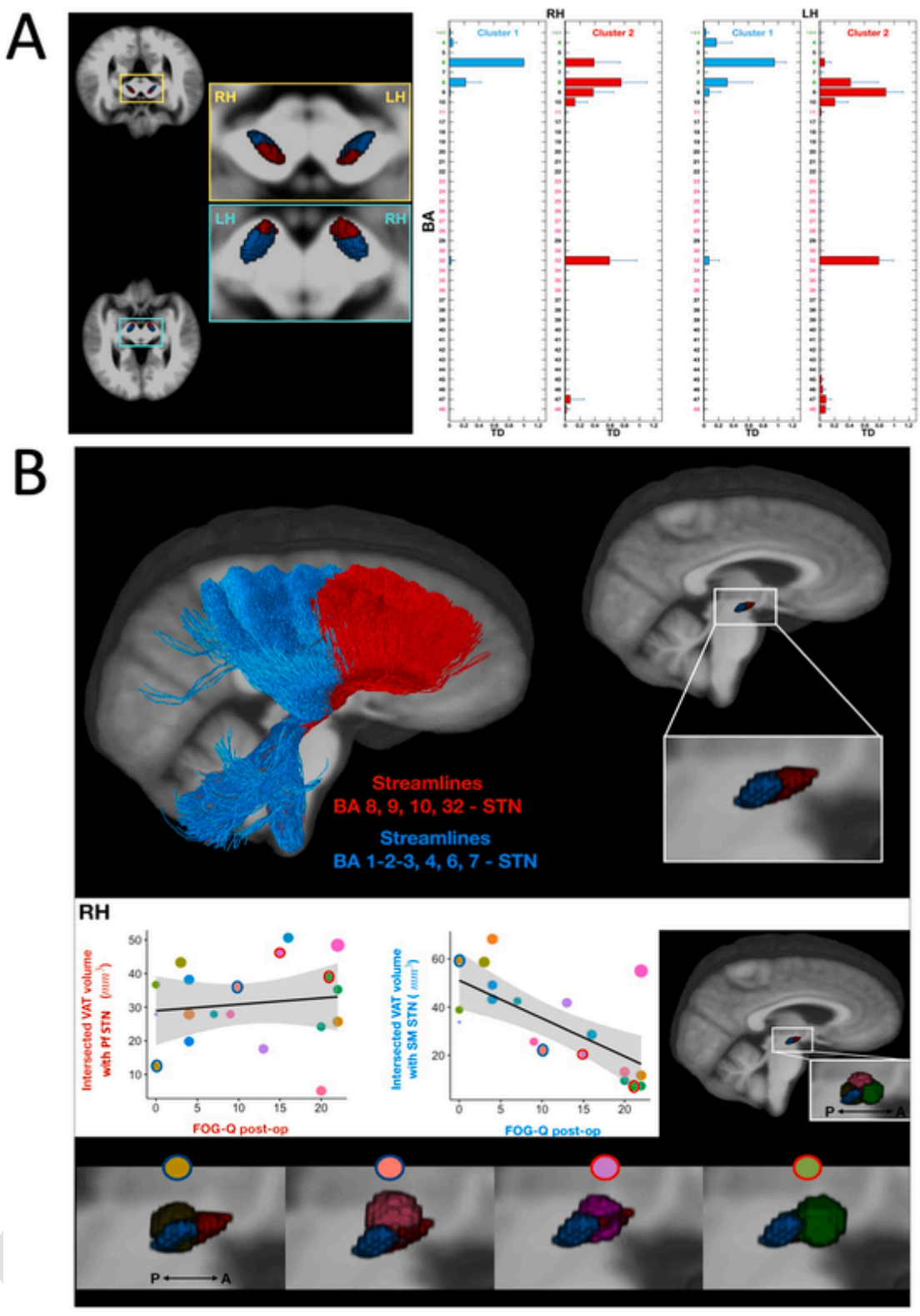

Fig. 3. Cortico-subthalamic clusters and relationship between intersected VAT with STN subdivisions and FOG severity.
A. Left panel: Subthalamic (STN) clusters obtained with hierarchical clustering from an anterior (top) and posterior (bottom) axial views. Right panel: histograms showing the connectivity profiles of the STN subdivisions with Brodmann areas (BA) which are outlined regarding their functions (sensorimotor in blue, associative in red and limbic in pink) on the y-axis and tract density values on the y-axis for respectively cluster 1 in blue and cluster 2 in red for RH and LH.B. Upper panel: cortico-STN streamlines arising from prefrontal cortical areas (red streamlines, BA 8,9,10,32), sensorimotor (BA 1-2-3, 4, 6) and parietal (BA 7) cortical areas (blue streamlines) and bipartition of the STN based on sensorimotor (blue) and prefrontal (red) STN connectivity. Bottom panel: Graphs showing bivariate relationship between the FOG-Q score and the volume of the intersected zone of the VATs with the Prefrontal (Pf) and sen-

◀ sorimotor (SM) clusters of the STN for the right hemisphere (RH). The regression line is in black and the confidence interval in grey, and each coloured dot represents individual VATs of each patient, and the dot size is proportional to its volume. Bottom panel: Examples of the VATs obtained in 4 patients with no (yellow dot), mild (pink dots) or severe postoperative FOG (green dot) and superimposed on the limbic (red) and sensorimotor (blue) clusters. (For interpretation of the references to colour in this figure legend, the reader is referred to the Web version of this article.)

in 22 patients, Castrioto et al. [38] observed no significant difference in the reduction of gait and axial scores when comparing the right and left STNs (25% with the right STN and 30% with the left STN for axial scores). In that study, it was however suggested that it was not the side of the hemisphere *per se* that impacts the most the effects of STN-DBS. Indeed, 8 patients had better effects on gait with unilateral left STN-DBS whereas only 3 patients had better effects on gait with unilateral right STN-DBS, thus not favoring the right STN as the best STN for gait disorders.

5. Limitations

Our study has some limitations. First, the number of patients included in this analysis is low even though we precisely analysed gait and balance prospectively and used validated clinical scales and gait recordings. In our study, we can also not fully rule out the role of a higher post-operative LEDD or other medication in the FOG severity after surgery, nor the role of lead implantation trajectories as previously reported for post-operative cognitive deficit [39]. However, we observed no significant post-operative cognitive deficit in any of the patients with post-operative FOG, and no obvious difference in other medication (see Table S2). The higher LEDD in these patients could mainly be the consequence of the less efficacy of STN-DBS on their gait problems (and not the cause) as we found no significant difference in the UPDRS III score with STN-DBS between freezers and non-freezers patients (see Table S1). Since these patients had no individual diffusion data, we used a normative tractogram of another cohort of PD patients, all candidates for STN DBS, with individual DWI to assess VAT connectivity. Our normative tractogram was obtained in a cohort of PD patients with similar clinical features suggesting that DWI results should be similar to PD patients already operated. Moreover, the use of normative tractograms could improve the signal to noise ratio for the connectivity assessment, but conversely it could smooth small individual differences. We also did not examine other fiber tracts that could be involved in gait control such as the GPe-STN, STN-GPi or STN-PPN [14], or functional connectivity profile [11]. Even though we used multi-shell diffusion data to improve diffusion signal modelling, these networks are difficult to isolate with high reliability due to the high numbers of crossing fibres. An improvement in tractogram reconstruction accuracy for quantitative analysis is still needed [40] together with methodological developments to explore small brain pathways using DWI *in vivo*.

6. Conclusion

Our study showed that the severity of FOG after surgery is related on the recruitment of the right cortico-subthalamic fibres, with lower FOG severity when VAT includes more sensorimotor and less prefrontal cortico-subthalamic fibres. This result could be important regarding the possibility for postoperative current shaping with the aim of improving FOG using directional DBS electrodes that could take into account individual modulations of these different cortico-subthalamic networks. Our study paves the way for the possibility in the near future to use DWI to provide additional individual information to refine surgical targeting, taking into account the precise topography of the cortical projections. However, higher resolution imaging approaches are now needed to propose individual anatomo-functional maps.

Financial support

This study was supported by the Institut National de la Santé et de la Recherche Médicale (INSERM, RBM C11-40), the program 'Investissements d'avenir' (ANR-10-IAIHU-06). Funding was provided by grants from the 'Institut du Cerveau et de la Moelle Epinière' (ICM) Foundation, the 'Régie Autonome des Transports Parisiens' (RATP), and the Agence Nationale de la Recherche (ANR-16-CE37-0007-02). Gizem Temiz and Marie des Neiges Santin received research funding support from Boston Scientific.

Authors' role

1. Research project: A. Conception: M-L Welter, C Karachi; B. Organization: G Temiz, A Collomb-Clerc, E Hainque, E Bardinet, M-L Welter, C Karachi; C. Execution: G Temiz, MdN Santin, C Olivier, A Collomb-Clerc, E Hainque, E Bardinet, S Fernandez-Vidal, B Lau, M-L Welter, C Karachi; 2. Statistical Analysis: G Temiz, B Lau; 3. Manuscript Preparation: A. Writing of the first draft: G Temiz, M-L Welter, C Karachi; B. Review and Critique: G Temiz, MdN Santin, C Olivier, A Collomb-Clerc, E Hainque, E Bardinet, S Fernandez-Vidal, B Lau, M-L Welter, C Karachi.

Declaration of competing interest

The Authors declare to have no conflict of interest relative to this research.

Acknowledgments

We are grateful to Anais Hervé and Clementine Trosch for their excellent patient care during the research trials, Angèle Van Hamme and Pasquale Varialle for helping in acquisition and analysis of gait data, and Hayat Belaid for neurosurgery assistance.

Appendix A. Supplementary data

Supplementary data to this article can be found online at https://doi.org/10.1016/j.parkreldis.2022.10.002.

References

[1] P. Limousin, P. Krack, P. Pollak, A. Benazzouz, C. Ardouin, D. Hoffmann, et al., Electrical stimulation of the subthalamic nucleus in advanced Parkinson's disease, N. Engl. J. Med. 339 (1998) 1105–1111.

[2] M.L. Welter, J.L. Houeto, S. Tezenas Du Montcel, V. Mesnage, A.M. Bonnet, B. Pillon, et al., Clinical predictive factors of subthalamic stimulation in Parkinson's disease, Brain 125 (2002), https://doi.org/10.1093/brain/awf050.

[3] A. Fasano, C.C. Aquino, J.K. Krauss, C.R. Honey, B.R. Bloem, Axial disability and deep brain stimulation in patients with Parkinson disease, Nat. Rev. Neurol. 11 (2015) 98–110 https://doi.org/nrneurol.2014.252 [pii]10.1038/nrneurol.2014.252.

[4] C. Karachi, F. Cormier-Dequaire, D. Grabli, B. Lau, H. Belaid, S. Navarro, et al., Clinical and anatomical predictors for freezing of gait and falls after subthalamic deep brain stimulation in Parkinson's disease patients, Park. Relat. Disord. 62 (2019) 91–97, https://doi.org/10.1016/j.parkreldis.2019.01.021.

[5] M.U. Ferraye, B. Debu, V. Fraix, J. Xie-Brustolin, S. Chabardes, P. Krack, et al., Effects of subthalamic nucleus stimulation and levodopa on freezing of gait in Parkinson disease, Neurology 70 (2008) 1431–1437 https://doi.org/70/16_Part_2/1431 [pii]10.1212/01.wnl.0000310416.90757.85.

[6] S. Vercruysse, W. Vandenberghe, L. Munks, B. Nuttin, H. Devos, A. Nieuwboer, Effects of deep brain stimulation of the subthalamic nucleus on freezing of gait in Parkinson's disease: a prospective controlled study, J. Neurol. Neurosurg. Psychiatry 85 (2014) 871–877 https://doi.org/jnnp-2013-306336 [pii]10.1136/jnnp-2013-306336.

[7] C. Moreau, L. Defebvre, A. Destee, S. Bleuse, F. Clement, J.L. Blatt, et al., STN-DBS frequency effects on freezing of gait in advanced Parkinson disease, Neurology 71 (2008) 80–84 https://doi.org/01.wnl.0000303972.16279.46 [pii]10.1212/01.wnl.0000303972.16279.46.
[8] P. Varriale, A. Collomb-Clerc, A. Van Hamme, A. Perrochon, G. Kemoun, G. Sorrentino, et al., Decreasing subthalamic deep brain stimulation frequency reverses cognitive interference during gait initiation in Parkinson's disease, Clin. Neurophysiol. 129 (2018) 2482–2491, https://doi.org/10.1016/j.clinph.2018.07.013.
[9] A. Horn, M. Reich, J. Vorwerk, N. Li, G. Wenzel, Q. Fang, et al., Connectivity Predicts deep brain stimulation outcome in Parkinson disease, Ann. Neurol. (2017), https://doi.org/10.1002/ana.24974.
[10] H. Akram, D. Georgiev, P. Mahlknecht, J. Hyam, T. Foltynie, P. Limousin, et al., Subthalamic deep brain stimulation sweet spots and hyperdirect cortical connectivity in Parkinson's disease, Neuroimage (2017), https://doi.org/10.1016/j.neuroimage.2017.07.012.
[11] L. Sobesky, L. Goede, V.J.J. Odekerken, Q. Wang, N. Li, C. Neudorfer, et al., Subthalamic and pallidal deep brain stimulation: are we modulating the same network? Brain 145 (2022) 251–262, https://doi.org/10.1093/brain/awab258.
[12] L.I. Boon, W.V. Potters, T.J.C. Zoon, O.A. van den Heuvel, N. Prent, R.M.A. de Bie, et al., Structural and functional correlates of subthalamic deep brain stimulation-induced apathy in Parkinson's disease, Brain Stimul. (2021), https://doi.org/10.1016/j.brs.2020.12.008.
[13] F. Irmen, A. Horn, P. Mosley, A. Perry, J.N. Petry-Schmelzer, H.S. Dafsari, et al., Left prefrontal connectivity links subthalamic stimulation with depressive symptoms, Ann. Neurol. (2020), https://doi.org/10.1002/ana.25734.
[14] J.N. Strelow, J.C. Baldermann, T.A. Dembek, H. Jergas, J.N. Petry-Schmelzer, F. Schott, et al., Structural connectivity of subthalamic nucleus stimulation for improving freezing of gait, J. Parkinsons Dis. (2022) https://doi.org/10.3233/JPD-212997, Apr 11.
[15] K. Ashkan, P. Rogers, H. Bergman, I. Ughratdar, Insights into the mechanisms of deep brain stimulation, Nat. Rev. Neurol. (2017), https://doi.org/10.1038/nrneurol.2017.105.
[16] N. Giladi, H. Shabtai, E.S. Simon, S. Biran, J. Tal, A.D. Korczyn, Construction of freezing of gait questionnaire for patients with Parkinsonism, Park. Relat. Disord. 6 (2000) 165–170 https://doi.org/S1353-8020(99)00062-0 [pii].
[17] N. Chastan, M.C. Do, F. Bonneville, F. Torny, F. Bloch, G.W.M. Westby, et al., Gait and balance disorders in Parkinson's disease: impaired active braking of the fall of centre of gravity, Mov. Disord. 24 (2009), https://doi.org/10.1002/mds.22269.
[18] O. Dergachyova, Y. Zhao, C. Haegelen, P. Jannin, C. Essert, Automatic preoperative planning of DBS electrode placement using anatomo-clinical atlases and volume of tissue activated, Int. J. Comput. Assist. Radiol. Surg. (2018), https://doi.org/10.1007/s11548-018-1724-8.
[19] G. Temiz, S.B. Sébille, C. Francois, E. Bardinet, C. Karachi, The anatomo-functional organization of the hyperdirect cortical pathway to the subthalamic area using in vivo structural connectivity imaging in humans, Brain Struct. Funct. (2020), https://doi.org/10.1007/s00429-019-02012-6.
[20] E. Moro, R.J. Esselink, J. Xie, M. Hommel, A.L. Benabid, P. Pollak, The impact on Parkinson's disease of electrical parameter settings in STN stimulation, Neurology 59 (2002) 706–713.
[21] A. Collomb-Clerc, M.-L. Welter, Effects of deep brain stimulation on balance and gait in patients with Parkinson's disease: a systematic neurophysiological review, Neurophysiol. Clin. 45 (2015), https://doi.org/10.1016/j.neucli.2015.07.001.
[22] A. Delval, C. Moreau, S. Bleuse, C. Tard, G. Ryckewaert, D. Devos, et al., Auditory cueing of gait initiation in Parkinson's disease patients with freezing of gait, Clin. Neurophysiol. 125 (2014) 1675–1681, https://doi.org/10.1016/j.clinph.2013.12.101.
[23] B.R. Bloem, Y.A. Grimbergen, J.G. van Dijk, M. Munneke, The "posture second" strategy: a review of wrong priorities in Parkinson's disease, J. Neurol. Sci. 248 (2006) 196–204, https://doi.org/10.1016/j.jns.2006.05.010.
[24] E. Heremans, A. Nieuwboer, S. Vercruysse, Freezing of gait in Parkinson's disease: where are we now? Curr. Neurol. Neurosci. Rep. 13 (2013) 350, https://doi.org/10.1007/s11910-013-0350-7.
[25] T.D. Parsons, S.A. Rogers, A.J. Braaten, S.P. Woods, A.I. Troster, Cognitive sequelae of subthalamic nucleus deep brain stimulation in Parkinson's disease: a meta-analysis, Lancet Neurol. 5 (2006) 578–588 https://doi.org/S1474-4422(06)70475-6 [pii]10.1016/S1474-4422(06)70475-6.
[26] M.H. Rosenbloom, J.D. Schmahmann, B.H. Price, The functional neuroanatomy of decision-making, J. Neuropsychiatry Clin. Neurosci. (2012), https://doi.org/10.1176/appi.neuropsych.11060139.
[27] J.M. Fuster, The prefrontal cortex in the neurology clinic, Handb. Clin. Neurol. (2019), https://doi.org/10.1016/B978-0-12-804281-6.00001-X.
[28] K. Bharti, A. Suppa, S. Tommasin, A. Zampogna, S. Pietracupa, A. Berardelli, et al., Neuroimaging advances in Parkinson's disease with freezing of gait: a systematic review, Neuroimage: Clinical (2019), https://doi.org/10.1016/j.nicl.2019.102059.
[29] C. Karachi, A. Andre, E. Bertasi, E. Bardinet, S. Lehericy, F.A. Bernard, Functional parcellation of the lateral mesencephalus, J. Neurosci. 32 (2012) 9396–9401 https://doi.org/32/27/9396 [pii]10.1523/JNEUROSCI.0509-12.2012.
[30] C.H. Lyoo, S. Aalto, J.O. Rinne, K.O. Lee, S.H. Oh, J.W. Chang, et al., Different cerebral cortical areas influence the effect of subthalamic nucleus stimulation on parkinsonian motor deficits and freezing of gait, Mov. Disord. 22 (2007) 2176–2182, https://doi.org/10.1002/mds.21609.
[31] J. Nonnekes, A.H. Snijders, J.G. Nutt, G. Deuschl, N. Giladi, B.R. Bloem, Freezing of gait: a practical approach to management, Lancet Neurol. 14 (2015) 768–778, https://doi.org/10.1016/S1474-4422(15)00041-1.
[32] M.J. Georgiades, J.M. Shine, M. Gilat, J. McMaster, B. Owler, N. Mahant, et al., Hitting the brakes: pathological subthalamic nucleus activity in Parkinson's disease gait freezing, Brain (2019), https://doi.org/10.1093/brain/awz325.
[33] V. Marchal, J. Sellers, M. Pelegrini-Issac, C. Gallea, E. Bertasi, R. Valabregue, et al., Deep brain activation patterns involved in virtual gait without and with a doorway: an fMRI study, PLoS One 14 (2019) e0223494, https://doi.org/10.1371/journal.pone.0223494.
[34] B.W. Fling, R.G. Cohen, M. Mancini, J.G. Nutt, D.A. Fair, F.B. Horak, Asymmetric pedunculopontine network connectivity in parkinsonian patients with freezing of gait, Brain 136 (2013) 2405–2418, https://doi.org/10.1093/brain/awt172.
[35] A. Fasano, J. Herzog, E. Seifert, H. Stolze, D. Falk, R. Reese, et al., Modulation of gait coordination by subthalamic stimulation improves freezing of gait, Mov. Disord. 26 (2011) 844–851, https://doi.org/10.1002/mds.23583.
[36] K.J. Lizárraga, B. Gnanamanogaran, T.M. Al-Ozzi, M. Cohn, G. Tomlinson, A. Boutet, et al., Lateralized subthalamic stimulation for axial dysfunction in Parkinson's disease: a randomized trial, Mov. Disord. 37 (2022) 1079–1087, https://doi.org/10.1002/mds.28953.
[37] S. Meoni, B. Debû, P. Pelissier, E. Scelzo, A. Castrioto, E. Seigneuret, et al., Asymmetric STN DBS for FOG in Parkinson's disease: a pilot trial, Park. Relat. Disord. 63 (2019) 94–99, https://doi.org/10.1016/j.parkreldis.2019.02.032.
[38] A. Castrioto, C. Meaney, C. Hamani, F. Mazzella, Y.-Y. Poon, A.M. Lozano, et al., The dominant-STN phenomenon in bilateral STN DBS for Parkinson's disease, Neurobiol. Dis. 41 (2011) 131–137, https://doi.org/10.1016/j.nbd.2010.08.029.
[39] K. Witt, O. Granert, C. Daniels, J. Volkmann, D. Falk, T. van Eimeren, et al., Relation of lead trajectory and electrode position to neuropsychological outcomes of subthalamic neurostimulation in Parkinson's disease: results from a randomized trial, Brain 136 (2013) 2109–2119 https://doi.org/awt151 [pii]10.1093/brain/awt151.
[40] R.E. Smith, F. Calamante, A. Connelly, Mapping connectomes with diffusion MRI: deterministic or probabilistic tractography? Magn. Reson. Med. (2020), https://doi.org/10.1002/mrm.27916.